An Analysis of The Electronic Properties of Monolayer Graphene and The Anomalous Quantum Hall Effect

Antoni Bandachowicz

University of Chicago

March 7th, 2023

Contents

1 Introduction

On an evening in the fall of 2002, Prof. Andre Geim of the University of Manchester and his group of graduate students became the first people to successfully isolate a two-dimensional

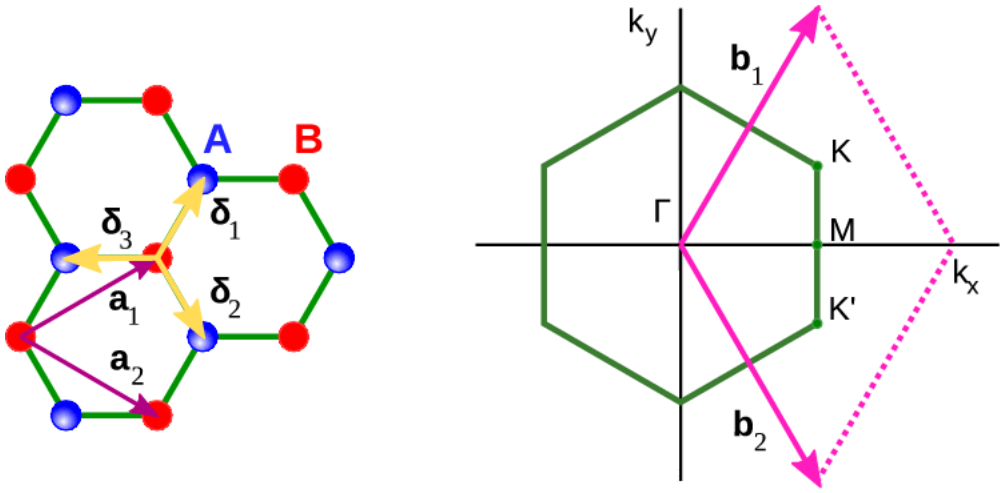

Figure 1: The basic lattice structure of graphene. The leftmost diagram demonstrates the geometry of lattice vectors and nearest-neighbor vectors. The rightmost diagram shows the Brillouin zone with the Dirac points K' and K located at the corners of the zone.

material: graphene. With nothing more than a sample of graphite and some scotch tape, Prof. Geim's group began the study of two-dimensional materials and their unique properties. This paper examines some of these unique properties of graphene, with a focus on the anomalous quantum Hall effect (AQHE). We start with a treatment of the elementary electronic properties of graphene, focusing on the monolayer, tight-binding approach. We will then move on to discuss the emergent pseudospin of low-energy electrons orbiting the Dirac points, and how this property leads to the Berry phase. We will finish with a derivation of the AQHE using a semiclassical model, and compare landau levels and Hall conductivity of AQHE and the integer quantum Hall effect (IQHE).

Ultimately, the goal of this paper is to give the reader an overview of a unique property of graphene while exploring the quantum Hall effect through an approach that was not covered in lecture.

2 An Analysis of The Graphene Monolayer

Graphene is an allotrope of carbon. It is a two-dimensional (2D) sheet of carbon atoms arranged in a hexagonal lattice, mimicking the shape of a honeycomb. This structure is illustrated in figure 1.

[1]

We can treat this lattice structure as a combination of two sub-lattices, denoted by the red and blue dots in the figure. We describe the sub-lattices using primitive lattice vectors, which we define as:

$$\mathbf{a}_1 = \frac{\sqrt{3}a}{2}(\sqrt{3}, 1) \tag{1}$$

$$\mathbf{a}_2 = \frac{\sqrt{3}a}{2}(\sqrt{3}, -1) \tag{2}$$

where a is the distance between neighboring atoms in graphene, which is roughly $a \approx 1.4 \times 10^{-10}$m. The choice of origin can be an arbitrary atom on the lattice. Sub-lattice A can be described using a linear combination of primitive lattice vectors

$$\mathbf{r} = n_1\mathbf{a}_1 + n_2\mathbf{a}_2 \tag{3}$$

where $n \in \mathbf{Z}$. Sub-lattice B can be described in terms of sub-lattice A such that

$$\mathbf{r} = n_1\mathbf{a}_1 + n_2\mathbf{a}_2 + \mathbf{d} \tag{4}$$

where $\mathbf{d} = (-a, 0)$ and $n \in \mathbf{Z}$. The reciprocal lattice vectors $\mathbf{b}_j$ representing the reciprocal space satisfy $\mathbf{b}_j \cdot \mathbf{a}_i = 2\pi\delta_{ij}$. We can therefore express them as:

$$\mathbf{b}_1 = \frac{2\pi}{3a}(1, \sqrt{3}) \tag{5}$$

$$\mathbf{b}_2 = \frac{2\pi}{3a}(1, -\sqrt{3}) \tag{6}$$

The reciprocal lattice is also triangular, rotated 90° from the original. We can find the first Brillouin zone (BZ) through the usual Weigner-Seitz process. The corners of the BZ, known as the Dirac points, are of particular interest to us due to unique physics we will discuss in later chapters. They are marked by K and K' in figure 1. Although the BZ is hexagonal with six corners, mathematically we view them as two sets of three corners. We can represent the inequivalent corners of the BZ in terms of reciprocal lattice vectors through the equations:

$$\mathbf{K} = \frac{1}{3}(2\mathbf{b}_1 + \mathbf{b}_2) \tag{7}$$

$$\mathbf{K'} = \frac{1}{3}(\mathbf{b}_1 + 2\mathbf{b}_2) \tag{8}$$

Finally, we introduce the nearest-neighbor vectors $\boldsymbol{\delta}$ to describe the lattice. These are of the form:

$$\boldsymbol{\delta}_1 = \frac{a}{2}(1, \sqrt{3}) \tag{9}$$

$$\boldsymbol{\delta}_2 = \frac{a}{2}(1, -\sqrt{3}) \tag{10}$$

$$\boldsymbol{\delta}_3 = -a(1, 0) \tag{11}$$

which are found by correctly assuming that the nearest-neighbor vectors are separated from each other by angles of $2\pi/3$ around the center atom.

3 Introducing the Tight-Binding Hamiltonian

We can describe the behavior of low-energy electrons within graphene's lattice structure using a tight-binding Hamiltonian. In more general approaches, the tight-binding Hamiltonian is derived from generalized Bloch equations and translational invariance. This approach can be found in Chapter 1 of McCann's textbook [2]. For simplicity, we will approach the tight-binding Hamiltonian using creation-annihilation operators.

Firstly, we assume that electrons can "hop" to nearest-neighbor atoms. By introducing a nearest-neighbor hopping energy $t \approx 2.8$eV we can write the Hamiltonian for the system as

$$\hat{H} = -t \sum_{ij} (\hat{a_i}^\dagger \hat{b_j} + \hat{b_j}^\dagger \hat{a_i}) \tag{12}$$

where i (j) labels sites in sub-lattice A(B), the fermionic operator $\hat{a_i}^\dagger$ ($\hat{a_i}$) creates (annihilates) an electron at the A site whose position is r_i, and similarly for $\hat{b_j}^\dagger$ ($\hat{b_j}$). At this point, we notice that a point on lattice B can be expressed in terms of position on lattice A and a nearest-neighbor vector such that $\boldsymbol{r_j} = \boldsymbol{r_i} + \boldsymbol{\delta}$. Therefore, we can re-write the Hamiltonian in equation 12 to incorporate summation over nearest-neighbors

$$\hat{H} = -t \sum_{ij} \sum_{\delta} (\hat{a_i}^\dagger \hat{b}_{i+\delta} + \hat{b}^\dagger_{i+\delta} \hat{a_i}) \tag{13}$$

Where the sum over δ is carried out over the three nearest-neighbor vectors described in the previous section. We can now rewrite the annihilation and creation operators in terms of their equivalents in momentum space (k-space), using

$$\hat{a_i}^\dagger = \frac{1}{\sqrt{N/2}} \sum_k e^{i\boldsymbol{k}\cdot\boldsymbol{r_i}} \hat{a_k}^\dagger \tag{14}$$

$$\hat{b_j} = \frac{1}{\sqrt{N/2}} \sum_{k'} e^{-i\boldsymbol{k'}\cdot(\boldsymbol{r_i}+\boldsymbol{\delta})} \hat{b_k} \tag{15}$$

where N/2 is the number of sites on the A,B sub-lattices. The other two operators can also be expressed in k-space in the same manner. This leads to a new expression of the Hamiltonian

$$\hat{H} = \frac{-t}{N/2} \sum_{i \in A} \sum_{\delta} (e^{i(\boldsymbol{k}-\boldsymbol{k'})\cdot \boldsymbol{r}_i} e^{-i\boldsymbol{k'}\cdot\boldsymbol{\delta}} \hat{a_k}^{\dagger} \hat{b_k} + H.c.). \tag{16}$$

We can use the relation between k and k' such that

$$\sum_{i \in A} e^{i(\boldsymbol{k}-\boldsymbol{k'})\cdot \boldsymbol{r}_i} = \frac{N}{2} \delta_{ij}. \tag{17}$$

And so,

$$\hat{H} = -t \sum_{\delta,k} (e^{-i\boldsymbol{k}\cdot\boldsymbol{\delta}} \hat{a_k}^{\dagger} \hat{b_k} + e^{i\boldsymbol{k}\cdot\boldsymbol{\delta}} \hat{b_k}^{\dagger} \hat{a_k}). \tag{18}$$

For convenience, we write the Hamiltonian in matrix form with

$$\hat{H} = \sum_{k} \boldsymbol{\Psi}^{\dagger} \boldsymbol{h}(\boldsymbol{k}) \boldsymbol{\Psi} \tag{19}$$

where,

$$\boldsymbol{\Psi} \equiv \begin{pmatrix} \hat{a}_{\mathbf{k}} \\ \hat{b}_{\mathbf{k}} \end{pmatrix}, \quad \boldsymbol{\Psi}^{\dagger} = \begin{pmatrix} \hat{a}^{\dagger}_{\mathbf{k}} & \hat{b}^{\dagger}_{\mathbf{k}} \end{pmatrix}$$

and

$$\mathbf{h}(\mathbf{k}) \equiv -t \begin{pmatrix} 0 & \Delta_{\mathbf{k}} \\ \Delta^{*}_{\mathbf{k}} & 0 \end{pmatrix}.$$

This is the matrix representation of the Hamiltonian, and it introduces the summations over the nearest-neighbor vectors as

$$\Delta_{\mathrm{k}} \equiv \sum_{\delta} e^{i\mathbf{k}\cdot\delta}$$

4 Energy Bands

We solve for the possible energies of this system using the standard eigen-problem process. Through $\begin{vmatrix} -\epsilon & \Delta_{\mathbf{k}} \\ \Delta^{*}_{\mathbf{k}} & -\epsilon \end{vmatrix} = 0$ we obtain the equation for the energy bands of graphene: $E_{\pm} = \pm t\sqrt{\Delta_{\mathbf{k}} \Delta^{*}_{\mathbf{k}}}$. By expanding out $\Delta_{\mathbf{k}}$ we get:

$$
\begin{aligned}
\Delta_{\mathbf{k}} &= e^{i\mathbf{k}\cdot\boldsymbol{\delta}_1} + e^{i\mathbf{k}\cdot\boldsymbol{\delta}_2} + e^{i\mathbf{k}\cdot\boldsymbol{\delta}_3} \\
&= e^{i\mathbf{k}\cdot\boldsymbol{\delta}_3}\left[1 + e^{i\mathbf{k}\cdot(\boldsymbol{\delta}_1-\boldsymbol{\delta}_3)} + e^{i\mathbf{k}\cdot(\boldsymbol{\delta}_2-\boldsymbol{\delta}_3)}\right] \\
&= e^{-ik_x a}\left[1 + e^{i3k_x a/2}e^{i\sqrt{3}k_y a/2} + e^{i3k_x a/2}e^{-i\sqrt{3}k_y a/2}\right] \\
&= e^{-ik_x a}\left[1 + e^{i3k_x a/2}\left(e^{i\sqrt{3}k_y a/2} + e^{-i\sqrt{3}k_y a/2}\right)\right] \\
&= e^{-ik_x a}\left[1 + 2e^{i3k_x a/2}\cos\left(\frac{\sqrt{3}}{2}k_y a\right)\right]
\end{aligned}
$$

Similarly, we have

$$
\Delta^*_{\mathbf{k}} = e^{ik_x a}\left[1 + 2e^{-i3k_x a/2}\cos\left(\frac{\sqrt{3}}{2}k_y a\right)\right]
$$

which leads to our expression of the energy bands

$$
E_{\pm}(\mathbf{k}) = \pm t\sqrt{1 + 4\cos\left(\frac{3}{2}k_x a\right)\cos\left(\frac{\sqrt{3}}{2}k_y a\right) + 4\cos^2\left(\frac{\sqrt{3}}{2}k_y a\right)}
$$

The positive (+) energy represents the conduction energy band, and the negative (-) energy represents the valence energy band. An interesting aspect of graphene is the fact that, in the nearest-neighbor approximation, the two energy bands are gapless and touch at the Dirac points. This means that the Dirac points are points where $E_{\pm}(\mathbf{k}) = 0$. Since the lower band is filled, the Fermi surface of graphene consists only of the Dirac points.

5 Behavior Near the Dirac Points

We can analyze the behavior of energy bands around the Dirac points by introducing a relative momentum term $\mathbf{q} \equiv \mathbf{k} - \mathbf{K}$. This allows us to write $\Delta_{\mathbf{k}}$ in terms of $\mathbf{q}$ as

$$
\begin{aligned}
\Delta_{\mathbf{K}+\mathbf{q}} &= e^{-iK_x a}e^{-iq_x a}\left[1 + 2e^{i3(K_x+q_x)a/2}\cos\left(\frac{\sqrt{3}\,(K_y+q_y)\,a}{2}\right)\right] \\
&= e^{-iK_x a}e^{-iq_x a}\left[1 - 2e^{3iaq_x/2}\cos\left(\frac{\pi}{3} + \frac{\sqrt{3}a}{2}q_y\right)\right].
\end{aligned}
$$

We now use the Taylor series expansion around the point $\mathbf{q} = \mathbf{0}$ to first order, which gives us

$$\Delta_{\mathbf{K}+\mathbf{q}} = -ie^{-iK_x a}\frac{3a}{2}\left(q_x + iq_y\right)$$

Similarly, we have

$$\Delta^*_{\mathbf{K}+\mathbf{q}} = ie^{iK_x a}\frac{3a}{2}\left(q_x - iq_y\right).$$

Since we have $E_\pm(\mathbf{K}+\mathbf{q}) = \pm t\sqrt{\Delta_{\mathbf{K}+\mathbf{q}}\Delta^*_{\mathbf{K}+\mathbf{q}}}$, we can ignore the phase term of both $\Delta_{\mathbf{K}+\mathbf{q}}$ and $\Delta^*_{\mathbf{K}+\mathbf{q}}$. We can therefore write the effective Hamiltonian for the behavior near the Dirac point $\boldsymbol{K}$ as

$$\mathbf{h}(\mathbf{K}+\mathbf{q}) = v_F\begin{pmatrix} 0 & q_x + iq_y \\ q_x - iq_y & 0 \end{pmatrix} \tag{20}$$

where

$$v_F = \frac{3at}{2} \approx 10^6 m/s.$$

Similarly, defining the relative momentum $\mathbf{q} \equiv \mathbf{k} - \mathbf{K}'$ and expanding $\Delta_{\mathbf{k}}$ about the Dirac point $\mathbf{K}'$, we find (dropping the phase term)

$$\Delta_{\mathbf{K}'+\mathbf{q}} = -\frac{3a}{2}\left(q_x - iq_y\right), \tag{21}$$

Which leads to a similar effective Hamiltonian to the one in equation 20

$$\mathbf{h}\left(\mathbf{K}'+\mathbf{q}\right) = v_F\begin{pmatrix} 0 & q_x - iq_y \\ q_x + iq_y & 0 \end{pmatrix}. \tag{22}$$

In these Hamiltonians, v_F is the Fermi velocity of graphene, and q_x and q_y are components of the relative crystal momentum measured from a Dirac point. In these Hamiltonians, the diagonal elements represent the "onsite" energy of electron residing completely on either the A or B atoms (they are defined as having zero energy). The off-diagonal elements represent the hopping of electrons from lattice A to B, and vice versa.

6 Linear Dispersion Relation

From the matrix Hamiltonians described in equations 20 and 22, we find that the energy bands near the Dirac points are described by

$$E_{\pm}(\mathbf{K}+\mathbf{q}) = E_{\pm}(\mathbf{K}'+\mathbf{q}) = E_{\pm}(\mathbf{q}) = v_F|\mathbf{q}| \tag{23}$$

This means that, near the Dirac point, the dispersion relation is linear in momentum. As a result, the energy bands form cones with centers lying on the Dirac points.

7 Bloch Functions

We have examined the unique behavior of energy bands of graphene and the linear dispersion relation in momentum space near the Dirac points. We can now move on to more implicit physics of the graphene lattice, most notably **pseudospin** and the **Berry phase** of electrons traveling in a closed loop near the Dirac points. These phenomena will give us an understanding of the emergence of the anomalous quantum hall effect. However, before we can look at these topics more carefully, we must first look at the formulation of possible wavefunctions describing our system. For this, we turn to Bloch functions. F. Bloch proved the theorem that the solutions of the schrödinger equation for a periodic potential must be of the form

$$\psi = U_q(r)e^{i\boldsymbol{q}\cdot\boldsymbol{r}}$$

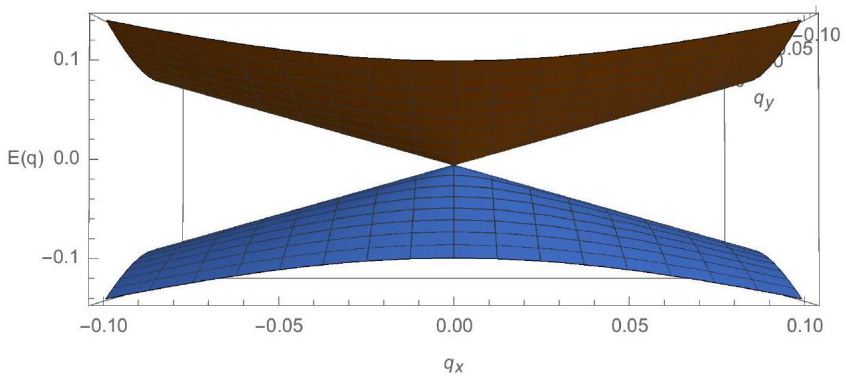

Figure 2: A linear dispersion relation near the Dirac points leads to Dirac cones with centers located on the edges of the BZ.

where $\boldsymbol{r}$ is the position vector with regards to some origin on the lattice. By inputting this periodic potential into $H\psi = E\psi$, where H and E are the effective Hamiltonian and the linear energy described above, we obtain

$$\psi_{\pm} = \frac{1}{\sqrt{2}} \begin{pmatrix} 1 \\ \pm e^{i\phi} \end{pmatrix} e^{i\mathbf{q}\cdot\mathbf{r}},$$

Note that we have now defined the relative momentum components as $q_x = q\cos\phi$ and $q_y = q\sin\phi$, where ϕ is the polar angle of the relative momentum in the graphene plane. This will be useful in our treatment of the Berry phase. The $\pm$ differentiates between the wavefunctions for the conduction (+) and valence (-) bands.

8 Pseudospin and Chirality in Graphene

From our derivation of our effective Hamiltonians and wavefunctions, we notice that both H and ψ have two components, which are reminiscent of spin-1/2. Focusing on $\psi_{\pm}$, the two-component vector part of $\psi_{\pm}$ is not related to the spin of the electron. Instead, by looking at our definition of the Bloch function, we see that this two-component vector shows the degree of freedom related to the relative amplitude of the Bloch function on the A or B sub-lattice. This degree of freedom is called pseudospin.

We can interpret the pseudospin vector component in the following manner. A spin-up state corresponds to all of the electronic density being located in the A sub-lattice, i.e

$$|\uparrow\rangle = \begin{pmatrix} 1 \\ 0 \end{pmatrix}$$

Whereas a spin-down state corresponds to all of the electronic density being located in the B sub-lattice, denoted

$$|\downarrow\rangle = \begin{pmatrix} 0 \\ 1 \end{pmatrix}$$

In reality, the electronic density is spread equally among both sub-lattices, differing only by a phase factor $e^{i\phi}$, leading to a linear combination of up and down states, lying within the plane of the graphene sheet.

8.1 Chirality

The electrons described by the $\psi_{\pm}$ wavefunction are also chiral. This means that the direction of the pseudospin is related to the direction of the relative momentum $\mathbf{q}$. This is clearly seen through the fact that the amplitude of $\psi_{\pm}$ is related to the polar momentum angle ϕ. For the Dirac point $\mathbf{K}$, the pseudospin in the conduction (+) band is parallel to the momentum, whereas the pseudospin in the valence (-) band is anti-parallel to it.

To see this relationship more clearly, we can introduce Pauli spin matrices σ in the A/B sub-lattice space. We can rewrite the effective Hamiltonian around the Dirac point $\mathbf{K}$ as

$$\mathbf{h}(\mathbf{K}+\mathbf{q}) = v_F \left(q_x\sigma_x - q_y\sigma_y\right) \tag{24}$$

Which we can simplify into the dot product

$$\mathbf{h}(\mathbf{K}+\mathbf{q}) = v_F\overline{\mathbf{q}}\cdot\boldsymbol{\sigma} \tag{25}$$

where we define the $\overline{\mathbf{q}}$ vector more explicitly as

$$\overline{\mathbf{q}} \equiv \begin{pmatrix} q_x \\ -q_y \\ 0 \end{pmatrix} = \begin{pmatrix} q\cos\phi \\ -q\sin\phi \\ 0 \end{pmatrix}.$$

Expressed in this way, the Pauli matrices $\boldsymbol{\sigma}$ now represent the pseudospin vector. The chiral operator $\overline{\mathbf{q}}\cdot\boldsymbol{\sigma}$ projects the pseudospin onto the direction of the relative momentum $\mathbf{q}$.

9 Berry Phase

The Berry phase θ is defined as the additional phase acquired by the eigenstate of an orbiting electron that is orbiting in a closed loop of constant energy. For graphene, one full rotation (at constant energy) of the relative momentum $\mathbf{q}$ of a low-energy electron around the Dirac point induces a phase in the eigenstate of the electron by a factor π. This is caused by our pseudospin term incorporated in the wavefunction. To see this, we derive the Berry phase

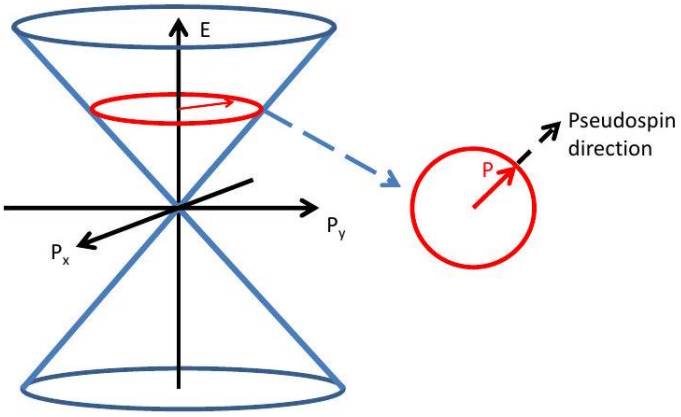

Figure 3: To obtain the Berry phase, we are integrating over a closed loop on the surface of the Dirac cone near the **K** Dirac point.

using the method described in [3].

$$\theta = -i \oint_C \left\langle \psi(\mathbf{q}(t)) \left| \frac{\partial}{\partial t} \right| \psi(\mathbf{q}(t)) \right\rangle dt$$

The integral is carried out as the relative momentum $\mathbf{q}$ is evolving in a closed circle C. Plugging in our Bloch wavefunction with pseudospin, we get

$$\theta = -i \oint_C dt \left[\frac{1}{2} \left(1, e^{-i\phi}\right) \begin{pmatrix} 0 \\ i\frac{\partial \phi}{\partial t} e^{i\phi} \end{pmatrix} + i \frac{\partial \mathbf{q}}{\partial t} \cdot \mathbf{r}/\hbar + i\mathbf{q} \cdot \frac{\partial \mathbf{r}}{\partial t}/\hbar \right]$$

Note that the second and third term in the integral are zero after integration over a closed loop. By considering the pseudospin term in the wavefunction, we get $\theta = \oint_C dt(\partial\phi/\partial t)/2 = \pi$. The complete mathematical motivation and formulation of the Berry phase and its relation to the pseudospin is more complicated and can be found in McCann's textbook [2], as well as in [4]. What is important to note, again, is that the rotation of the relative momentum of the low-energy electron around the Dirac point induces a phase π. Notably, in this semi-classical model, the circular motion of the low-energy electron is normally caused by a magnetic field being applied to the lattice. Therefore, the introduction of a magnetic field acting on a graphene monolayer will cause a phase π in the eigenstates describing the electrons within the energy bands. This will give rise to anomalous energy for the landau-levels describing our graphene system, which in turn will give rise to the anomalous IQHE.

10 A simplified connection between the Berry Phase and the Anomalous QHE

We know that a magnetic field perpendicular to the plane of the graphene lattice will make low-energy electrons near the Dirac points travel in closed loops around the points. This motion will create a Berry phase, which in turn is responsible for the zero energy Landau level (LL). This zero energy LL causes a shift in Hall plateaux, which leads to altered plateaux in conductivity and thus the anomalous quantum hall effect. Below we demonstrate how the Berry phase leads to anomalous energies for the LL.

To derive the anomalous energies, we use a semiclassical model of the behavior of electrons near the Dirac point. This method is known as Onsager's semiclassical derivation of Landau Levels for electrons in solids [5]. When a magnetic field is applied, electrons are forced to move in circular orbits. Classically, any radius is allowed. However, in the semiclassical approach, we invoke the Bohr-Sommerfield quantization rule. This rule ensures the electron wavefunctions are single-valued. In short, the quantization rule states that the path integral of the electron's momentum over a closed orbit is equal to an integer multiple of Planck's constant, which we can write as

$$\oint d\mathbf{r} \cdot \mathbf{q}/\hbar = 2\pi n \tag{26}$$

where n is a non-negative integer. For electrons in a magnetic field (with a vector potential $\mathbf{A}$), the relative momentum of the circulating electron can be written in terms of the crystal momentum $\mathbf{k}$ as $\mathbf{q} = \hbar\mathbf{k} - e\mathbf{A}$, which can be interpreted as a type of canonical momentum in the presence of gauge field $\mathbf{A}$. Plugging our momentum back into the quantization rule, we obtain

$$(\hbar \oint d\mathbf{r} \cdot \mathbf{k} - e \oint d\mathbf{r} \cdot \mathbf{A})/\hbar = 2\pi n. \tag{27}$$

Next, we can rewrite the Lorentz force law for a particle traveling in a magnetic field as $\hbar\dot{\mathbf{k}} = -e\dot{\mathbf{r}} \times \mathbf{B}$, which, when integrating with respect to time, gives

$$\hbar\mathbf{k} = -e\mathbf{r} \times \mathbf{B} + \text{ constant } . \tag{28}$$

Plugging equation 28 back into the first term of equation 27, we get

$$-e\mathbf{B} \cdot \oint d\mathbf{r} \times \mathbf{r} = 2e\Phi$$

where Φ is the magnetic flux of the orbit under the field B. Using Stokes' theorem, the second term of equation 27 can be written as $e\int d\mathbf{S}\cdot\nabla\times\mathbf{A} = e\Phi$. Therefore, we can rewrite and simplify equation 27 such that

$$\Phi = \frac{nh}{e} \tag{29}$$

where h/e is the flux quantum. We see that the quantization rule leads to a quantization condition for the flux in real space. The magnetic flux threading the orbit of an electron should be quantized to an integer times the flux quantum [3]. Using our definition of magnetic flux $\phi = \iint \mathbf{B}\cdot d\mathbf{S}$ where the surface area is the circle mapped by the rotation of $\mathbf{q}$, we can rewrite the flux as

$$\pi k^2 = 2\pi neB/\hbar. \tag{30}$$

Applying this condition to the free electron gas, we get the energy quantization rule

$$E_n = \hbar^2k^2/2m = n\hbar eB/m = n\hbar\omega_C \tag{31}$$

where ω_C is the cyclotron frequency. This is the simplest possible result, without considering behavior at $E_0 = 1/2\hbar\omega_C$ (the zero-point energy) and without considering the Berry phase. In order to consider the zero-point energy we need to introduce the Maslov index. This is a purely quantum mechanical effect that the semiclassical model does not capture, so we add it manually. In our in-class treatment of the quantum Hall effect, the zero-point energy emerged naturally from the fact that our system simplified to the harmonic oscillator under the landau gauge. In this oversimplified treatment, this is not the case. We can rewrite the Bohr-Sommerfeld quantization condition of equation 27 to account for the zero-point energy

$$(\hbar\oint d\mathbf{r}\cdot\mathbf{k} - e\oint d\mathbf{r}\cdot\mathbf{A})/\hbar = 2\pi(n+1/2). \tag{32}$$

Now let us consider the full quantization rule for graphene, meaning we consider the Berry phase phenomenon. When the momentum $\mathbf{q}$ of an electron is forced to evolve in a circle, in addition to the normal phase factors of $\oint d\mathbf{r}\cdot\mathbf{k}$ and $e\oint d\mathbf{r}\cdot\mathbf{A}/\hbar$, it also acquires an extra Berry phase of π. So our quantization rule should be

$$(\hbar\oint d\mathbf{r}\cdot\mathbf{k} - e\oint d\mathbf{r}\cdot\mathbf{A})/\hbar + \pi = 2\pi(n+1/2). \tag{33}$$

Noticeably, the Berry phase cancels the Maslov index. So the final quantization rule in momentum space for graphene is the same as equation 30. Since the dispersion relation for

graphene is linear such that $E = v_F|\mathbf{q}|$ (where q is the relative momentum near the Dirac point, which we can treat as k in equation 30), the Landau level energy for graphene is ($\hbar = 1$

$$E_n = v\sqrt{2neB}. \tag{34}$$

This equation for the energy of the Landau levels allows for zero energy. This altered energy creates a shift in the plateaux for the Hall conductivity, leading to the anomalous QHE. A comparison of Hall conductivities for materials with and without the Berry phase is shown in figure 4.

It is clear that this semiclassical approach to the anomalous QHE is oversimplified. The energies for the Landau levels and Hall conductivity are usually found by starting with a Landau density, which sums over possible iterations of Dirac spinors, which in turn describe all of the degrees of freedom of the system with the inclusion of the pseudospin. A review of this technique can be found in [6]. When the system is properly formulated and assessed, we get the following relationship for the Hall conductivity:

$$\sigma_{xy} = -\frac{1}{2}(2n+1)(\frac{4e^2}{h}). \tag{35}$$

Diagram (b) in figure 4 plots the conductivity found in equation 35. At zero energy, meaning where $n = 0$, a step in σ_{xy} of size $\frac{4e^2}{h}$ is created instead of the plateau found in diagram (a). Therefore, a significant difference between the anomalous QHE (AQHE) and the integer quantum Hall effect (IQHE) in other materials is the difference in Hall conductivity. It is important to note that the step sizes between the two phenomena also differ. The distance between each σ_{xy} step for AQHE on the density axis in figure 4 is $4Be/h$, meaning the steps occur at integer values of $4Be/h$. The distance between steps in diagram (a) is gBe/h, where g is some degeneracy of the system.

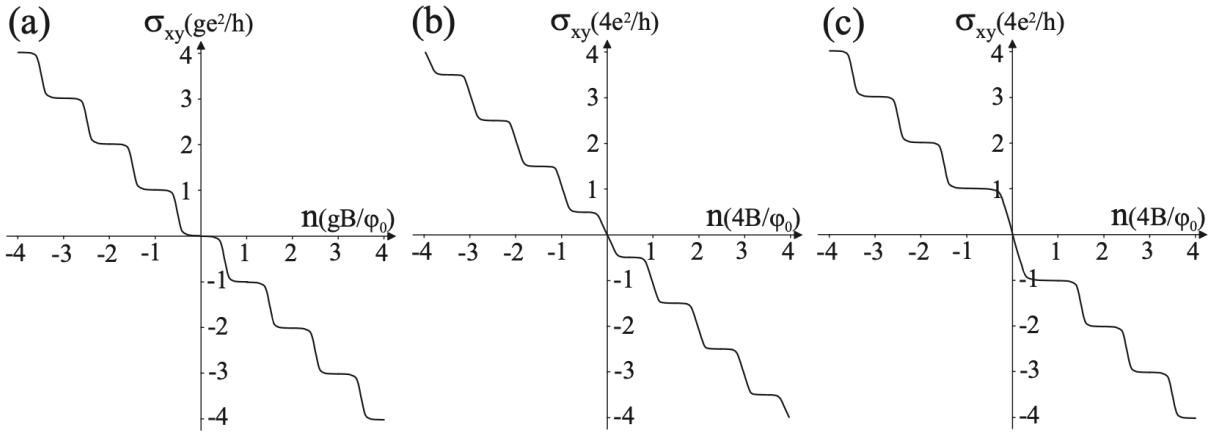

Figure 4: three types of integer quantum Hall effect, showing the density dependence of the Hall conductivity $\sigma_{xy}(n)$: (a) conventional two-dimensional semiconductor systems with some additional system degeneracy g; (b) monolayer graphene; (c) bilayer graphene. Here, B is the magnitude of the magnetic field and $\phi_0 = \mathrm{h/e}$ is the flux quantum.[2]

11 Conclusion

In this paper, we explored the anomalous quantum Hall effect emerging from the electronic properties of monolayer graphene. We started with a tight-binding hamiltonian describing the behavior of low-energy electrons interacting with the hexagonal lattice of graphene. We then moved on to describe the energy bands and their behavior around the Dirac points. This allowed us to examine pseudospin properties emergent in the eigenstates of low-energy electrons near the Dirac points, and how this pseudospin is responsible for the Berry Phase. Finally, we showed that the Berry phase influences the Landau levels using Onsager's over-simplified model, and we compared the Hall conductivity of AQHE and IQHE.

References

[1] Jia-Ming Liu and I-Tan Lin. *Basic Properties and Band Structure*, page 1–26. Cambridge University Press, 2018.

[2] Edward McCann. Electronic properties of monolayer and bilayer graphene. In *Graphene Nanoelectronics*, pages 237–275. Springer Berlin Heidelberg, 2011.

[3] Jiamin Xue. Berry phase and the unconventional quantum hall effect in graphene, 2013.

[4] Cheol-Hwan Park and Nicola Marzari. Berry phase and pseudospin winding number in bilayer graphene. *Phys. Rev. B*, 84:205440, Nov 2011.

[5] J. N. Fuchs, F. Piéchon, M. O. Goerbig, and G. Montambaux. Topological berry phase and semiclassical quantization of cyclotron orbits for two dimensional electrons in coupled band models. *The European Physical Journal B*, 77(3):351–362, sep 2010.

[6] V. P. Gusynin and S. G. Sharapov. Unconventional integer quantum hall effect in graphene. *Phys. Rev. Lett.*, 95:146801, Sep 2005.